Nature of optical transitions involving cation vacancies and complexes in AlN and AlGaN

A. Sedhain, J. Y. Lin, and H. X. Jiang

Citation: Appl. Phys. Lett. **100**, 221107 (2012); doi: 10.1063/1.4723693
View online: http://dx.doi.org/10.1063/1.4723693
View Table of Contents: http://apl.aip.org/resource/1/APPLAB/v100/i22
Published by the American Institute of Physics.

Nature of optical transitions involving cation vacancies and complexes in AlN and AlGaN

A. Sedhain, J. Y. Lin, and H. X. Jiang[a)]
Department of Electrical and Computer Engineering, Texas Tech University, Lubbock, Texas 79409, USA

(Received 18 April 2012; accepted 14 May 2012; published online 30 May 2012)

Photoluminescence spectroscopy was employed to probe the nature of optical transitions involving Al vacancy (V_{Al}) and vacancy-oxygen complex (V_{Al}-O_N) in AlN. An emission line near 2 eV due to the recombination between the 2− charge state of $(V_{Al}\text{-}O_N)^{2-/1-}$, and the valence band was directly observed under a below bandgap excitation scheme. This photoluminescence (PL) band was further resolved into two emission lines at 1.9 and 2.1 eV, due to the anisotropic binding energies of V_{Al}-O_N complex caused by two different bonding configurations–the substitutional O_N sits along c-axis or sits on one of the three equivalent tetrahedral positions. Moreover, under an above bandgap excitation scheme, a donor-acceptor pair like transition involving shallow donors and $(V_{Al}\text{-}O_N)^{2-/1-}$ deep acceptors, which is the "yellow-luminescence" band counterpart in AlN, was also seen to split into two emission lines at 3.884 and 4.026 eV for the same physical reason. Together with previous results, a more complete picture for the optical transitions involving cation vacancy related deep centers in AlGaN alloy system has been constructed. © *2012 American Institute of Physics*. [http://dx.doi.org/10.1063/1.4723693]

Al-rich AlGaN and AlN have been the subject of intense research effort during the last decade due to their applications in deep ultraviolet (DUV) photonics,[1–5] surface acoustic wave (SAW) devices,[6,7] and field emitters.[8] The superior physical and chemical properties of AlN, such as ultra-wide direct bandgap,[9,10] high melting point,[11] high thermal conductivity,[12] mechanical strength, and radiation hardness, miscibility with GaN in the entire alloy region, make it technologically important. AlN based photodetectors with a cut-off wavelength at 207 nm and extremely low dark current[13] and p-i-n homojunction DUV light emitting diode with emission peak around 210 nm[14] have been reported. AlGaN based DUV emitters operating at 250–280 nm with quantum efficiency of about 3% have been achieved.[3]

In addition to the deepening of donor and acceptor levels in $Al_xGa_{1-x}N$ with x, another factor that limits the doping efficiency in Al-rich AlGaN is the formation of native defects and their complexes, such as Al vacancy (V_{Al}) and V_{Al}-oxygen complex (V_{Al}-O_N). These defects offer electronic levels deep inside the bandgap. Incorporation of impurities (Si or O) further lowers the formation energy of such defects through the shift of Fermi level position. These deep level centers act as single to triple electron traps and, therefore, are partly responsible for low n-type conductivity observed in Si-doped AlN and Al-rich AlGaN alloys.[15–18] Furthermore, the presence of native point defect recombination centers is responsible in part for the reduced DUV emission efficiency in AlN.[19] Understanding the electronic structure of native point defects and their complexes is important to further improve the material quality and, consequently, improve the performance of AlGaN based devices.

The well-known yellow-luminescence (YL) band in GaN has been extensively studied. This band is believed to be a donor-acceptor-pair (DAP) type transition from a shallow donor to a deep acceptor. First principal calculations, positron annihilation, and doping experiments strongly suggest that the deep acceptor is a complex consisting of a gallium vacancy and a nearest neighbor donor, an oxygen atom sitting on one of the neighboring nitrogen sites $(V_{Ga}\text{-}O_N)^{2-/1-}$.[20–26] Two different configurations of $(V_{Ga}\text{-}O_N)^{2-/1-}$, which arise due to Ga-N bond anisotropy, with O_N along the c-axis (axial configuration) or in one of the three equivalent tetrahedral positions (basal configuration), were directly observed via visible and infrared (IR) photoluminescence (PL) spectroscopy studies.[18] In this Letter, we report the direct observation of the YL-band counterpart in AlN and its corresponding band-to-impurity transition involving $(V_{Al}\text{-}O_N)^{2-/1-}$ and the valence band (VB) by employing both below and above bandgap excitation schemes. Our results suggest the equivalent "YL-band" is due to donor-acceptor like recombination between a shallow donor and 1− charge state of $(V_{Al}\text{-}O_N)^{2-/1-}$, while the observed IR emission line is due to the recombination between electrons in the 2− charge state of $(V_{AlN}\text{-}O_N)^{2-/1-}$ and free holes. Both lines were observed to further split into two fine structures due to the Al-N bond anisotropy. The details of AlN epilayers and the DUV PL system used in this study were described elsewhere.[15–17]

Figure 1(a) shows a 300 K PL spectrum of AlN measured from 1.6 to 6.2 eV under an above bandgap excitation ($\lambda_{exc} = 195$ nm). In the near band edge region, two emission lines at ~5.95 eV and ~5.84 eV were observed. We attribute these lines to the free exciton recombination and the associated longitudinal optical (LO) phonon replica, with an LO phonon energy of 110 meV in AlN.[21] Two impurity bands were observed; one near 2.76 eV and the other consisting of two lines at 3.884 and 4.026 eV. Emission band near 2.76 eV has been discussed exclusively in a previous work and assigned to the recombination between electrons in the

[a)]Electronic mail: hx.jiang@ttu.edu.

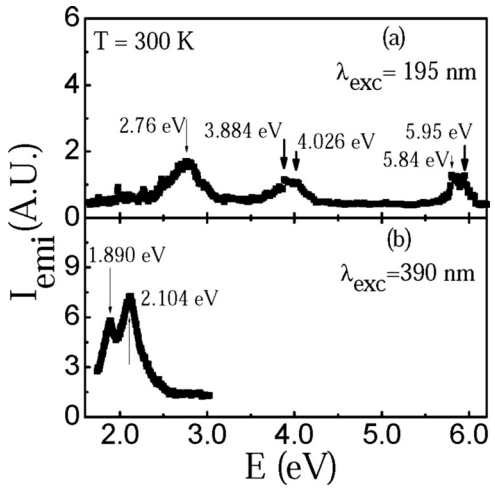

FIG. 1. Room temperature (300 K) PL spectra of AlN under excitation by (a) above bandgap (195 nm) and (b) below bandgap (390 nm) photons.

3– charge state of isolated Al vacancies ($V_{Al}^{3-/2-}$) and free holes in the valence band.[17]

An impurity related emission band ~3.9 eV region was previously observed in AlN and identified to have a similar physical origin as the YL band in GaN (~2.2 eV); both involving the transition from shallow donor to $(V_{III}\text{-}O_N)^{2-/1-}$. Based on the fact that the YL band in GaN was resolved into two lines due to the anisotropic binding energies of V_{Ga}-O_N complex depending on whether the substitutional oxygen sits in π- (when O_N sits along c-axis) or σ- (when O_N sits on one of the three equivalent tetrahedral positions) bonding configuration,[18] the transition in AlN with the same physical origin is equally prone to splitting into two lines. Therefore, we suggest that the two emission lines near 3.884 and 4.026 eV in Fig. 1(a) arise from the splitting of a previously observed line near 3.9 eV.[16]

In order to further investigate the nature of the two emission lines at 3.884 and 4.026 eV in AlN, we performed PL measurements under below bandgap excitation. As illustrated in Fig. 1(b), under a below bandgap excitation scheme ($\lambda_{exc} = 390$ nm ≈ 3.18 eV), two peaks at 1.890 and 2.104 eV emerge. Figure 2(a) shows the temperature dependent PL spectra under below bandgap excitation measured from 10 to 350 K. The Arrhenius plots for the integrated PL intensity of both peaks (near 1.88 and 2. 09 eV at 10 K) are shown in Fig. 2(b) and described by

$$I(T) = I(0)[1 + ae^{-E_0/KT}]^{-1}, \quad (1)$$

where I(T) and I(0) represent the PL intensity at temperature T and at 0 K, a is a constant, E_0 is a characteristic thermal activation energy of PL intensity, and k is Boltzmann constant. The fitted values of E_0 are 59.9 and 54.2 meV for 1.88 and 2.09 eV lines, respectively. The very similar E_0 values suggest that these two emission lines are of the same physical origin.

Based on the PL emission spectrum obtained under the above bandgap excitation scheme in Fig. 1(a), the energy level of the deep acceptor $(V_{Al}\text{-}O_N)^{2-/1-}$ in AlN lies about 2.06 eV (≈5.96–3.9 eV) above the valence band maximum. Taking the Al-N bond anisotropy into account, spectral line due to the recombination between the electrons in the 2− charge state of $(V_{Al}\text{-}O_N)^{2-/1-}$ and free holes is expected to be resolved into two lines with slightly different energies. Therefore, we suggest that the observed spectral lines at 1.890 and 2.104 eV are due to the recombination between free holes and electrons in the 2− charge state of $(V_{Al}\text{-}O_N)^{2-/1-}$ with two different bonding configurations.

Figure 3(a) shows an illustration of π- and σ-bonding configurations of V_{Al}-O_N complex in AlN. We believe that this bonding anisotropy is responsible for the splitting of both emission bands near 3.9 eV in Fig. 1(a) and 2.0 eV in Fig. 1(b) observed in the above bandgap and below bandgap excitation schemes, respectively. Accordingly, an energy level diagram for AlN at 300 K can be constructed and is shown in Fig. 3(b), illustrating the electronic levels of 2- and 1− charge states of $(V_{Al}\text{-}O_N)^{2-/1-}$, as well as the fine structures arising from Al-N bond anisotropy.

In the below band-gap excitation scheme, the 1– charge state of $(V_{Al}\text{-}O_N)^{2-/1-}$ can accept one more electron from the valence band and changes itself to 2– charge state, $(V_{Al}\text{-}O_N)^{2-}$. The 2− charge state of $(V_{Al}\text{-}O_N)^{2-/1-}$ participates in the PL emission through the recombination with free holes

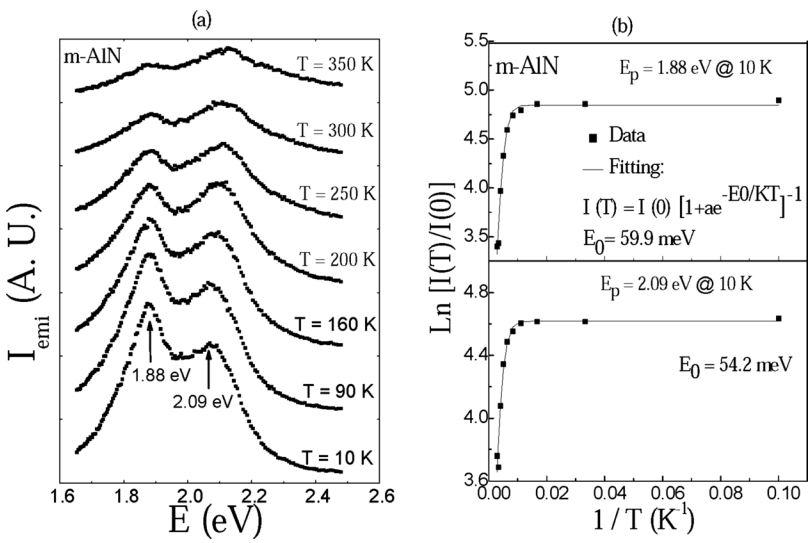

FIG. 2. (a) Temperature dependent PL spectra of AlN from 1.65 to 2.5 eV spectral region under below bandgap (390 nm) excitation. (b) The Arrhenius plot of the PL emission intensity of 1.88 (top) and 2.09 (bottom) eV lines in AlN. PL data are shown as the solid squares, and the solid lines are the least squares fit of data with Eq. (1).

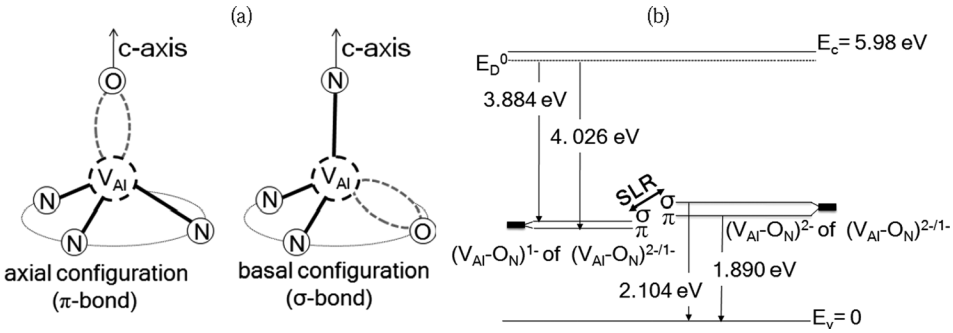

FIG. 3. (a) Illustration of electronic structures of the $(V_{Al}\text{-}O_N)^{2-/1-}$ complex in AlN for oxygen replacing the nitrogen from π-bonding (along c-axis) and σ-bonding (one of the other three equivalent positions) configurations. (b) Energy level diagram of AlN including $(V_{Al}\text{-}O_N)^{2-/1-}$ center with the charge states $(V_{Al}\text{-}O_N)^{2-}$ and $(V_{Al}\text{-}O_N)^{1-}$. SLR stands for small lattice relaxation. The top of the valence band is considered to be the reference zero energy level.

and subsequently changes itself back to the 1– charge state via a small lattice relaxation. Certain number of $(V_{Al}\text{-}O_N)^{1-}$ defects are expected to exist in our AlN samples. This is because the populations of different charge states are determined by their formation energies and charge neutrality. Another route for free hole generation is via excitation of electrons from the valence band to the 2– charge state of $V_{Al}^{3-/2-}$. This is plausible because the below band-gap excitation energy we employed (~3.18 eV) is also sufficient to create more 2– charge states of $V_{Al}^{3-/2-}$ by raising electrons from the 3– charge states of $V_{Al}^{3-/2-}$ to the conduction band, assuming the recombination rate for $(V_{Al}\text{-}O_N)^{2-} \rightarrow$ VB transition (~2.0 eV) is higher than $V_{Al}^{3-} \rightarrow$ VB transition (~2.76 eV) under the below bandgap excitation scheme.

Based on the above discussion and Fig. 3(b), the observed PL emission lines in AlN related to $(V_{Al}\text{-}O_N)^{2-/1-}$ can be described by the following set of equations:

$$D^0+(V_{Al}-O_N^{\sigma})^{1-} = D^+ + (V_{Al}-O_N^{\sigma})^{2-} + h\nu(3.884\ \text{eV}), \quad (2)$$

$$D^0 + (V_{Al}-O_N^{\pi})^{1-} = D^+ + (V_{Al}-O_N^{\pi})^{2-} + h\nu(4.026\ \text{eV}), \quad (3)$$

$$(V_{Al}-O_N^{\sigma})^{2-} + h^+ = (V_{Al}-O_N^{\sigma})^{1-} + h\nu(2.104\ \text{eV}), \quad (4)$$

$$(V_{Al}-O_N^{\pi})^{2-} + h^+ = (V_{Al}-O_N^{\pi})^{1-} + h\nu(1.890\ \text{eV}), \quad (5)$$

where D^0 and D^+ denote the neutral and ionized donors, respectively.

Our previous studies have demonstrated that the energy levels of deep acceptors, $(V_{III})^{3-/2-}$ and $(V_{III}\text{-complex})^{2-/1-}$, in $Al_xGa_{1-x}N$ ($0 \le x \le 1$) alloys, are pinned to a common energy level in vacuum.[15,16] Based on the present and previous results, we have constructed a more complete picture for describing the optical transitions involving deep centers in AlGaN alloys. In constructing Fig. 4, conduction (E_C) and valence (E_V) band edges as functions of Al-content are derived from the compositional dependence of the bandgap, $E_g(x) = xE_g(AlN) + (1-x)E_g(GaN) - bx(1-x)$, where b is the bowing parameter (1 eV for AlGaN alloys). Room temperature band gaps of GaN and AlN were taken as 3.42 eV and 6.05 eV, respectively. Conduction and VB offset parameters have been considered to be 0.70 and 0.30, respectively. The top of the VB of GaN is a reference zero level.

From Fig. 4, we expect that there should be a total of three transition lines involving deep centers and VB. Except $V_{Al}^{3-/2-}$, the other two should have fine structure splitting due to the Ga (Al)–N bond anisotropy of wurtzite crystal structure. The downward arrow on lower right side shows the 2.78 eV transition involving $V_{Al}^{3-/2-}$ in AlN.[17] Table I summarizes possible transitions related to the deep acceptor-like centers in AlN observed in this work and reported previously. Two charge states of each of these deep centers are indicated. Taking the Al-N bond anisotropy into account, spectral lines related to each charge state further split into two fine structures, which are designated with π and σ. Table I indicates that the acceptor level of $(V_{Al}\text{-}2O_N)^{1-/0}$ in AlN is about 5.96–4.7 eV≈1.26 eV. Thus, in addition to the transitions already observed, it may be possible to observe more transition lines in the 1.2–1.3 eV spectral region in AlN with O incorporation.

In summary, a PL emission band in AlN near 2.0 eV arising from the recombination between deep acceptor-like centers, $(V_{Al}\text{-}O_N)^{2-/1-}$, and free holes has been observed in a below bandgap excitation scheme. This emission line was further resolved into two spectral lines at 1.890 and 2.104 eV. The splitting results from the different binding energies of $V_{Al}\text{-}O_N$ complex with the bond orientation along and perpendicular to the crystal c-axis. Moreover, under an above bandgap excitation scheme, the "yellow-luminescence" band counterpart in AlN involving shallow donors and $(V_{Al}\text{-}O_N)^{2-/1-}$ deep acceptors was also seen to split into two emission lines at 3.884 and 4.026 eV for the same physical reason. The present work together with our previous reports[15–18] provides a more complete picture on the optical transitions involving cation vacancies and complexes in AlN and AlGaN.

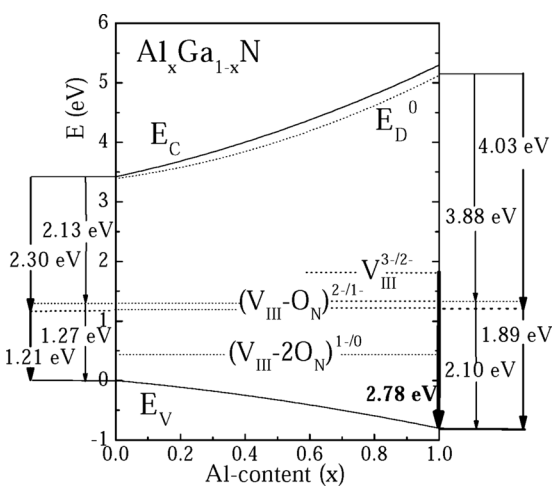

FIG. 4. Deep center $(V_{III}\text{-}O_N)^{2-/1-}$ related DAP and band-to-impurity transition lines observed in GaN and AlN plotted together with $V_{III}^{3-/2-}$ and $(V_{III}\text{-}2O_N)^{1-/0}$ levels and E_V, E_C, and E_D^0 as functions of Al-content.

TABLE I. Summary of the PL emission energies related to the deep centers in AlN including their various charge states and effect of Al-N bond anisotropy of π and σ configurations. SLR stands for small lattice relaxation.

Defect (deep center)	Charge State	Configuration	Transition energy (eV) with D^0	Transition energy (eV) with h^+ (VB)	σ-π energy splitting (meV)	Comment
$V_{Al}^{3-/2-}$	V_{Al}^{3-}			2.78		
	V_{Al}^{2-}		3.4			SLR ~0.10 eV
$(V_{Al}\text{-}O_N)^{2-/1-}$	$(V_{Al}\text{-}O_N)^{2-}$	σ		2.104	214	
		π		1.890		SLR ~0.08 eV
	$(V_{Al}\text{-}O_N)^{1-}$	σ	3.884		142	
		π	4.026			
$(V_{Al}\text{-}2O_N)^{1-/0}$	$(V_{Al}\text{-}2O_N)^{1-}$	σ		not reported		
		π				
	$(V_{Al}\text{-}2O_N)^0$	σ (π) not-resolved	4.70			

This work is supported by DOE under Grant No. DE-FG02-09ER46552. Jiang and Lin are grateful to the AT&T Foundation for the support of Ed Whitacre and Linda Whitacre Endowed Chairs.

[1]H. X. Jiang and J. Y. Lin, in *AlN Epitaxial Layers for UV Photonics*, edited by M. Razeghi and M. Henini (Elsevier, Oxford, 2004), chap. 7.
[2]A. Khan, K. Balakrishnan, and T. Katona, Nature Photon. **2**, 77 (2008).
[3]C. Pernot, M. Kim, S. Fukahori, T. Inazu, T. Fujita, Y. Nagasawa, A. Hirano, M. Ippommatsu, M. Iwaya, S. Kamiyama, I. Akasaki, and H. Amano, Appl. Phys. Exp. **3**, 061004 (2010).
[4]M. Kneissl, Z. Yang, M. Teepe, C. Knollenberg, O. Schmidt, P. Kiesel, N. M. Johnson, S. Schujman, and L. J. Schowalter, J. Appl. Phys. **101**, 123103 (2007).
[5]R. T. Bondokov, S. G. Mueller, K. E. Morgan, G. A. Slack, S. Schujman, M. C. Wood, J. A. Smart, and L. J. Schowalter, J. Cryst. Growth **310**, 4020 (2008).
[6]O. Elmazria, V. Mortet, M. El Hakiki, M. Nesladek, P. Alnot, and U. H. Pomcare, IEEE Transc. Ultrason. Ferroelectr. Freq. Control **50**, 710 (2003).
[7]T. Aubert, O. Elmazria, B. Assouar, L. Bouvot, and M. Oudich, Appl. Phys. Lett. **96**, 203503 (2010).
[8]Y. B. Tang, H. T. Cong, Z. M. Wang, and H. M. Cheng, Appl. Phys. Lett. **89**, 253112 (2006).
[9]W. M. Yim, E. J. Stofko, P. J. Zanzucchi, J. I. Pankove, M. Ettenberg, and S. L. Gilbert, J. Appl. Phys. **44**, 292 (1972).
[10]J. Li, K. B. Nam, M. L. Nakarmi, J. Y. Lin, H. X. Jiang, P. Carrier, and S. H. Wei, Appl. Phys. Lett. **83**, 5163 (2003).
[11]G. Yu, in *Properties of Advanced Semiconductor Materials GaN, AlN, InN, BN, SiC, SiGe*, edited by M. E. Levinshtein, S. L. Rumyantsev, and M. S. Shur (Wiley, New York, 2001), pp. 31–47.
[12]G. A. Slack, R. A. Tanzilli, R. O. Pohl, and J. W. Vandersande, J. Phys. Chem. Sol. **48**, 641 (1987).
[13]J. Li, Z. Y. Fan, R. Dahal, M. L. Nakarmi, J. Y. Lin, and H. X. Jiang, Appl. Phys. Lett. **89**, 213510 (2006).
[14]Y. Taniyasu, M. Kasu, and T. Makimoto, Nature (London) **441**, 325 (2006).
[15]N. Nepal, M. L. Nakarmi, J. Y. Lin, and H. X. Jiang, Appl. Phys. Lett. **89**, 092107 (2006).
[16]K. B. Nam, M. L. Nakarmi, J. Y. Lin, and H. X. Jiang, Appl. Phys. Lett. **86**, 222108 (2005).
[17]A. Sedhain, L. Du, J. H. Edgar, J. Y. Lin, and H. X. Jiang, Appl. Phys. Lett. **95**, 262104 (2009).
[18]A. Sedhain, J. Y. Lin, and H. X. Jiang, Appl. Phys. Lett. **96**, 151902 (2010).
[19]S. F. Chichibu, T. Onuma, K. Hazu, and A. Uedono, Appl. Phys. Lett. **97**, 201904 (2010).
[20]S. Limpijumnong and C. G. Van de Walle, Phys. Rev. B **69**, 035207 (2004).
[21]T. Mattila and R. M. Nieminen, Phys. Rev. B **55**, 9571 (1997).
[22]I. Gorczyca, N. E. Christensen, and A. Svane, Phys. Rev. B **66**, 075210 (2002).
[23]K. Saarinen, T. Laine, S. Kuisma, J. Nissilä, P. Hautojärvi, L. Dobrzynski, J. M. Baranowski, K. Pakula, R. Stepniewski, M. Wojdak, A. Wysmolek, T. Suski, M. Leszczynski, I. Grzegory, and S. Porowski, Phys. Rev. Lett. **79**, 3030 (1997).
[24]J. Oila, V. Ranki, J. Kivioja, K. Saarinen, P. Hautojärvi, J. Likonen, J. M. Baranowski, K. Pakula, T. Suski, M. Leszczynski, and I. Grzegory, Phys. Rev. B **63**, 045205 (2001).
[25]A. Uedono, S. F. Chichibu, Z. Q. Chen, M. Sumiya, R. Suzuki, T. Ohdaira, and T. Mikado, J. Appl. Phys. **90**, 181 (2001).
[26]K. Saarinen, V. Ranki, T. Suski, M. Bockowski, and I. Grzegory, J. Cryst. Growth **246**, 281 (2002).